Journal of Coastal Research	SI	95	1201–1205	Coconut Creek, Florida	2020

Importance of Wave Non-linearity for 3D Morphodynamic Modelling

Baptiste Mengual[†*], Xavier Bertin[†], and Kévin Martins[†‡]

[†]UMR 7266 LIENSs
CNRS-La Rochelle University
La Rochelle, France

[‡]UMR 5805 EPOC
CNRS Bordeaux University
Bordeaux, France

www.cerf-jcr.org

www.JCRonline.org

ABSTRACT

Mengual, B.; Bertin, X., and Martins, K., 2020. Importance of wave non-linearity for 3D morphodynamic modelling. *In:* Malvárez, G. and Navas, F. (eds.), *Global Coastal Issues of 2020. Journal of Coastal Research*, Special Issue No. 95, pp. 1201-1205. Coconut Creek (Florida), ISSN 0749-0208.

The effect of wave non-linearity on morphological changes of a sandbar is investigated through a realistic application at Duck Beach (North Carolina, USA) of a 3D state-of-the-art process-based morphodynamic model, which couples sediment transport, currents and waves (vortex force formalism). From simplified 1D/2DH models, previous studies highlighted that acceleration skewness of non-breaking waves over a sandbar could promote its progressive onshore migration. This process can counterbalance the offshore migration occurring under breaking waves through the development of strong offshore-directed "undertow" currents near the seabed. Based on the existing literature, an additional bedload flux associated to acceleration skewness of waves is implemented in the 3D model. Numerical experiments with and without this additional term clearly demonstrate the need to account for this supplementary wave-induced transport to reproduce onshore migration phases of the sandbar. Effectively, even a model integrating wave asymmetry effects on bedload flux estimates and 3D wave-current interactions fails to reproduce the observed onshore migration of the sandbar.

ADDITIONAL INDEX WORDS: *Morphodynamics, wave non-linearity, onshore sandbar migration.*

INTRODUCTION

Waves play a key role in sediment remobilization and transport in nearshore environments like beaches or inlets (*e.g.,* longshore transport caused by littoral drift, cross-shore exchanges; *e.g.* see Dodet *et al.,* 2013). Nearshore sandbars are commonly found in the nearshore zone along wave-exposed sandy coasts, with different morphologic features depending on local hydrodynamics (Short, 1979). They act as natural protections of beaches against waves by reducing the incoming energy through depth-induced breaking. For instance, sandbars can reduce wave-induced processes close to the coast (*e.g.* wave run-up), which substantially contribute to coastal inundation and erosion issues (Sallenger, Holman, and Birkemeier, 1985).

In the past decades, many studies focused on the processes controlling their cross-shore dynamics. During energetic wave conditions, intense wave breaking on the bar crest was shown to result in a strong near-bed and offshore-directed flow, *i.e.,* the so-called "undertow", driving a quick offshore migration (*O*(10 m/day)) of sandbars (Gallagher, Elgar, and Guza, 1998). During mild wave conditions, *i.e.,* when wave breaking over the bar is absent, a progressive onshore migration (*O*(1 m/day)) was often reported in observations. Elgar Gallagher, and Guza (2001) identified the acceleration skewness associated with non-linear shoaling waves as the driver of this onshore sediment transport resulting in a shoreward migration of sandbars. Indeed, over the bar, waves become asymmetric and exhibit pitched-forward shapes with steep front faces generating large accelerations that promote sediment transport towards the shore. Using process-based phase-averaged models of beach profile evolutions, several studies succeeded in reproducing onshore migration phases of sandbars through the integration of an additional sediment flux term, which is function of wave acceleration skewness (hereafter Q_a; *e.g.,* see Dubarbier *et al.,* 2015; Hoefel and Elgar, 2003; Ruessink *et al.,* 2007). Dubarbier *et al.* (2015) evaluated the respective contributions of mean currents, bed slopes, and velocity and acceleration skewness on morphological evolutions of different barred beaches, and highlighted the key role of wave acceleration to reproduce onshore migration phases. However, previous modelling studies were generally restricted to 1D/2DH applications. To our knowledge, the Q_a contribution in a 3D application based on a state-of-the-art morphodynamic model accounting for sediment transport and wave/current interactions has never been investigated.

In this study, realistic 3 week-long simulations are performed during the DUCK94 experiment (Gallagher, Elgar, and Guza, 1998) at Duck Beach (North Carolina, USA). After a presentation of the study site and the 3D numerical modelling system, several simulations accounting or not for Q_a are performed in order to assess its contribution on sediment fluxes and subsequent morphological changes over the Duck Beach sandbar.

METHODS

General Outline of the Numerical Modelling System

The hydrodynamic core of the morphodynamic modelling system is based on the Semi-Implicit Cross-scale Hydroscience

DOI: 10.2112/SI95-233.1 received 31 March 2019; accepted in revision 13 February 2020.
*Corresponding author: bapt.mengual@hotmail.fr
©Coastal Education and Research Foundation, Inc. 2020

Integrated System Model (SCHISM) of Zhang *et al.* (2016). SCHISM solves the 3D Reynolds-averaged Navier-Stokes in its hydrostatic form on unstructured grid. An Eulerian-Lagrangian Method is combined with semi-implicit schemes to treat the advection term in the momentum equations, which relaxes the numerical stability constraints and authorizes the CFL numbers to be well above 1. Regarding the turbulence closure, the vertical viscosity and diffusivity terms are derived from the General Ocean Turbulence Model (GOTM; Umlauf and Burchard, 2005), using a *k-ε* model.

SCHISM is coupled with the Wind Wave Model (WWM) of Roland *et al.* (2012), a third-generation spectral wave model that simulates gravity waves generation and propagation by solving the wave action equation. Three-dimensional wave-induced circulations and wave-current interactions are taken into account using a vortex-force formalism (Ardhuin, Rascle, and Belibassakis, 2008), implemented in SCHISM by Guérin *et al.* (2018). Depth-induced breaking is modelled using the approach of Van der Westhuysen (2010), who uses the biphase to define the breaker fraction and the breaking criterion (threshold value set at $-4\pi/9$).

Regarding sediment dynamics, suspended and bedload transport and subsequent bed morphological changes are simulated using the sediment module of Pinto *et al.* (2012). Suspended sediment transport is computed by solving an advection-diffusion equation, taking advantage of the recent development of a high-order implicit advection scheme (TVD^2) in SCHISM. The implicit treatment in the vertical dimension enables to considerably reduce computational costs associated with the large settling velocity of sediments and vertical advection in the presence of steep slopes. Bedload fluxes are estimated according to the formalism of Soulsby and Damgaard (2005), which enables relevant estimates in presence of current plus asymmetric waves. In our implementation, orbital velocity skewness effects are computed following the approach of Elfrink, Hanes, and Ruessink (2006). The resulting bed changes are computed by solving the sediment continuity/Exner equation with a Weighted Essentially Non-Oscillatory scheme (WENO; Guérin, Bertin, and Dodet, 2016) that prevents the development of numerical oscillations in the bed without adding diffusion or filters.

Wave-induced Sediment Transport caused by Acceleration Skewness

Sediment fluxes caused by wave-induced acceleration Q_a are computed according to the procedure of Dubarbier *et al.* (2015) and Ruessink, Ramaekers, and Van Rijn (2012)

$$Q_a = -K_a\left(A_u A_w\right) \;\; if \; A_w > A_{crit} \tag{1}$$

with the velocity asymmetry coefficient A_u and the near-bed acceleration amplitude A_w expressed as

$$A_u = \frac{0.857}{1+\exp\left(\frac{-0.471-\log\left(U_r\right)}{0.297}\right)}\sin\left(-\frac{\pi}{2}+\frac{\pi}{2}\tanh\left(\frac{0.815}{U_r^{\;0.672}}\right)\right) \tag{2}$$

$$A_w = \omega\frac{\pi H_{rms}}{T_p \sinh\left(kh\right)} \tag{3}$$

where U_r refers to the Ursell number, H_{rms} to the root-mean-square wave height, T_p to the peak wave period, and ω to the angular frequency ($2\pi/T_p$). The calibration coefficient K_a and the critical acceleration A_{crit}, above which Q_a is considered, are respectively set at 1.4×10^{-4} and 0.2 m.s^{-2}, according to Hoefel and Elgar (2003). In case of $A_w > A_{crit}$, Q_a is considered as an additional bedload flux oriented in the mean wave direction.

Duck Beach configuration and hydrodynamic validation

The model configuration for Duck Beach, illustrated on Figure 1, is characterized by an horizontal resolution varying from 25 m offshore to 4 m in the nearshore area, and 20 equidistant σ-layers along the vertical.

This study focuses on the 21st September/ 12th October 1994 period corresponding to the DUCK94 experiment (Gallagher, Elgar, and Guza, 1998) during which many data acquisitions were conducted at the U.S. Army Corps of Engineers Field Research Facility at Duck (North Carolina), defining a cross-shore section at the longshore position 930 m (hereinafter *Sec930*; Figure 1b). This extensive dataset includes measurements of water levels, winds, currents, wave spectra and bathymetry and is used to force and validate the model. Forcing conditions throughout the period of interest are illustrated on Figure 2. Elevation and directional wave spectra measurements acquired at 8 m depth are used as offshore boundary conditions for SCHISM and WWM, respectively. Both models are run with the same time step fixed at 15 s. Regarding sediment dynamics, only one sediment class of 250 μm is considered. A skin roughness $z_0=2.5\times10^{-5}$ m is used to compute bed shear stress. For suspension, the erosion rate is set at 3.4×10^{-3} kg/m^2/s (Wu and Lin, 2014), the critical shear stress at 0.16 N/m^2, and the settling velocity at 3.3 cm/s (Soulsby, 1997).

The hydrodynamic validation of the model is performed on the 12th October during energetic wave conditions in terms

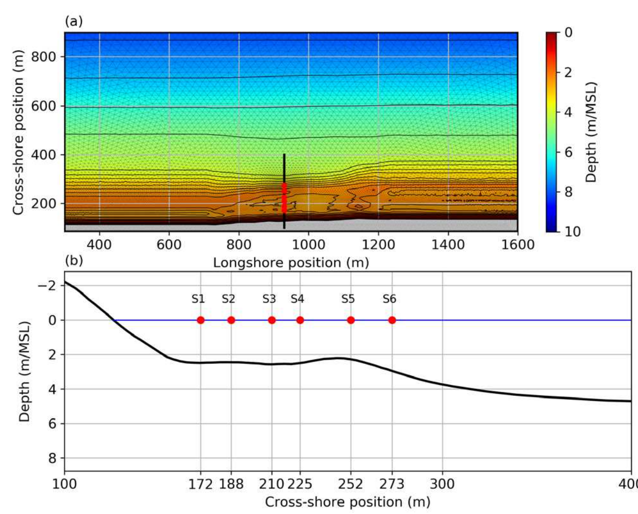

Figure 1. (a) Duck Beach model configuration with its initial bathymetry on the 21st September 1994 (with respect to Mean Sea Level) and its unstructured grid; (b) Initial cross-shore profile of bathymetry at longshore position 930 m (*Sec930*), along which model results are validated and discussed in terms of morphological changes. Red dots refer to measurement stations (*S1* to *S6*) where model-data comparisons are provided. Black contours on (a) correspond to isobaths (every 0.25 m from 0 to 4 m depth, every meter for larger depths).

of significant wave height (H_s) and vertical profiles of cross-shore currents at different stations along *Sec930* (Figure 3). This comparison reveals good predictive skills both in terms of H_s (Root Mean Squared Difference, RMSD, of 0.1 m; RMSD normalized by the mean value, NRMSD, of 6.24 %) and cross-shore currents, despite an underestimation in the vertical shear of current at *S3* and *S4*, a problem already faced by several authors like Moghimi *et al.* (2013).

Numerical Experiment

Thereafter, the focus is on morphological evolutions of the sandbar along *Sec930* (Figure 1b) occurring between the 21st and the 30th September. A first simulation, considered as a reference (hereinafter R_{ref}), is performed without the additional bedload term Q_a due to acceleration skewness of waves. A second one, R_{Qa}, includes this new sediment flux. In the next section, results from both simulations are compared to observed bathymetric changes over the same period.

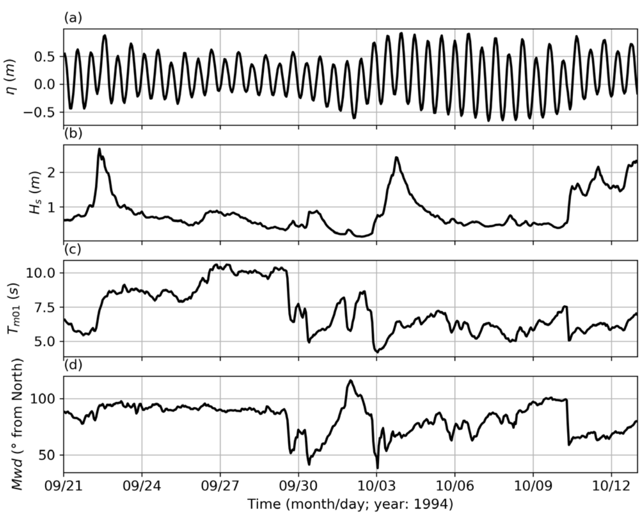

Figure 2. Offshore conditions along the simulated period in terms of (a) sea surface elevation η, (b) significant wave height H_s, (c) mean wave period T_{m01}, and (d) mean wave direction *Mwd*.

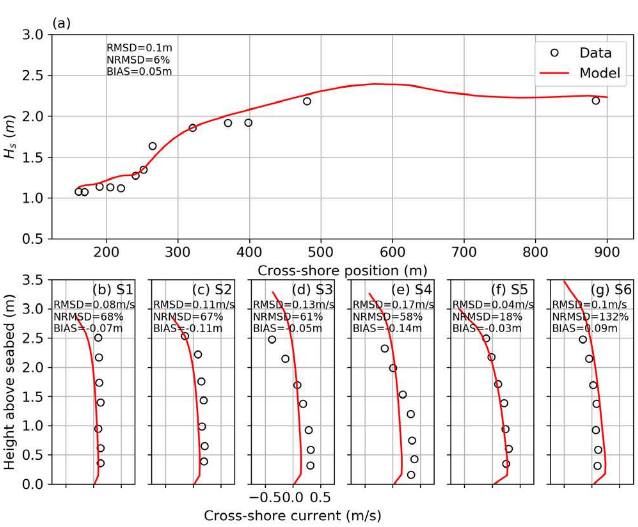

Figure 3. Hydrodynamic validation on the 12th October 1994 (energetic conditions) along *Sec930* (see location on Figure 1): (a) H_s (19:00, UTC; high tide, η=0.71 m); (b) to (g) vertical profiles of cross-shore currents at stations *S1* to *S6*. Current profiles correspond to different times (UTC): *S1*, 22:21 (η=0.16 m); *S2*, 21:12 (η=0.45 m); *S3*, 19:40 (η=0.685 m); *S4*, 18:27 (η=0.715 m); *S5*, 17:10 (η=0.65 m); *S6*, 15:30 (η=0.335 m).

RESULTS

Morphological evolutions of the sandbar derived from the two simulations accounting or not for Q_a (R_{Qa} and R_{ref}, respectively) are compared to bathymetric observations at 3 different dates (21st, 24th, and 30th of September; see Figure 4).

Based on field observations, a clear onshore migration of the sandbar by about 20 m is highlighted between the 9/21 and the 9/30 (Figure 4a), which corresponds to a mean migration rate of approximatively 2 m.day^{-1}. Until the 9/24, this shoreward dynamics is moderate but it clearly intensifies during the following days.

The R_{ref} simulation (no Q_a) does not follow this observed trend in bed changes (negative Brier Skill Score, BSS; Sutherland, Peet, and Soulsby, 2004), and only exhibits a very slight offshore displacement of the bar (Figure 4b). On the opposite, the onshore migration of the sandbar is well captured in the R_{Qa} simulation accounting for Q_a (BSS=0.6), with a migration rate of 1-2 m.day^{-1}, consistent with observations (Figure 4c).

Contrasted morphological changes derived from the two simulations are explained by large differences in the magnitude and the residual orientation of bedload sediment fluxes. In R_{ref}, bedload fluxes computed according to the formulation of Soulsby and Damgaard (2005), $Q_{b,SD}$, remain weak and generally oriented offshore over the bar (<0.02 kg/m/s near the bar crest; see blue curve on Figure 5c). In simulation R_{Qa}, the supplementary flux Q_a added to $Q_{b,SD}$ actually dominates the latter most of the time with an opposite direction (red curve on Figure 5c). Near the bar crest, the dominance of Q_a is clear with an average onshore flux of -0.02 kg/m/s over the 9/21-9/30 period, about 15 times higher than the average $Q_{b,SD}$.

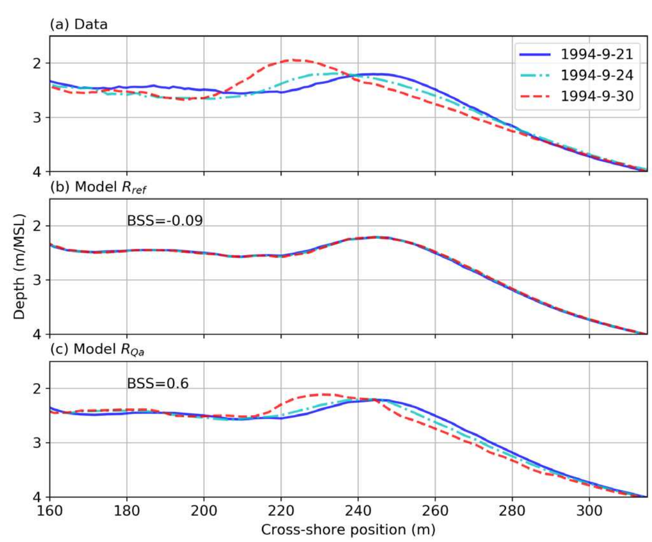

Figure 4. Bathymetry evolution over the sandbar (on each subplot, the different curves depict different dates): (a) observed; (b) derived from simulation R_{ref} (without Q_a); (c) derived from simulation R_{Qa} (with Q_a).

Despite relevant results provided by R_{Qa} simulation, some noticeable differences remain between modelled and measured bed evolutions. In model results, accretion over the bar crest is underestimated by 50%. In addition, erosion occurring between cross-shore positions 180 and 200 m is not reproduced by the model. These model shortcomings are commented in the discussion section.

DISCUSSION

Analysis of Model Shortcomings

Local erosion/deposition patterns on both sides of the sandbar result from a subtle compromise between fluxes caused by near-bed undertow currents and those driven by wave asymmetry and acceleration skewness, in particular during moderate wave conditions. The underestimated accretion over the bar crest simulated by the model at the end of September in comparison with observations (red curves on Figure 4) can be related to weaker undertow currents simulated between stations *S3* and *S4* (Figures 3d and 3e). The underestimation of the undertow at these two stations also corresponds to a region where the dissipation of short waves is underestimated by roughly 20 %. While the approach of Van der Westhuysen (2010) resulted in considerable improvement for wave height prediction compared to classical models like Battjes and Janssen (1978), further efforts are needed to improve the representation of wave dissipation locally, such as in the bar trough. Interestingly, this underestimation increases when the critical acceleration (A_{crit}) considered in Q_a estimates (Eq. 1) is set to 0 instead of 0.2 m.s^{-2} (Figure 6). This means that the A_{crit} threshold promotes bedload fluxes induced by near-bed currents which result in substantial bed changes, even during moderate wave conditions dominated by Q_a.

Model shortcomings could be tackled in different manners in future works. Regarding wave modelling, a potential way to improve model predictions of undertow currents would be to account for a wave roller model, which was already identified as a contributor in the vertical shear of cross-shore current profiles (Moghimi *et al.,* 2013). For sediment dynamics, considering only one sediment class is probably too restrictive and may impact the simulated morphological changes. Given the heterogeneity in bed sediments measured at Duck Beach along cross-shore profiles (Gallagher *et al.,* 2016), model results should be improved by including several classes (from fine to very coarse sediments), with an initial bed condition representing the cross-shore sediment sorting.

Importance of Q_a in Nearshore Morphodynamic Applications

Processes controlling onshore sandbar migration are not well known compared to those driven offshore migration (Elgar, Gallagher, and Guza, 2001; Fernandez-Mora *et al.,* 2015). By considering the acceleration skewness in sediment transport formulations, some studies demonstrated the capacity of process-based models to reproduce the onshore migration of sandbars (*e.g.,* Dubarbier *et al.,* 2015; Fernandez-Mora *et al.,* 2015; Hoefel and Elgar, 2003; Ruessink *et al.,* 2007). However, these models generally correspond to 1D/2DH applications where the transport owing to undertow is parameterized and which do not account for 3D wave-current interactions. 3D model results from the present study underline the need of accounting for acceleration skewness to reproduce sandbar dynamics. This motivates further researches based on 3D approaches to assess morphological evolutions driven by this process in complex nearshore environments. In particular, several studies showed that the dynamics of ebb-delta sandbars that develop at the mouth of tidal inlets and estuaries was dominated by onshore-directed flows, driven by short wave dissipation (Bertin, Fortunato, and Oliveira, 2009; Ridderinkhof *et al.,* 2016). However, these studies neglected the contribution of wave asymmetry and acceleration, which certainly have a key contribution on the dynamics of these sandbars.

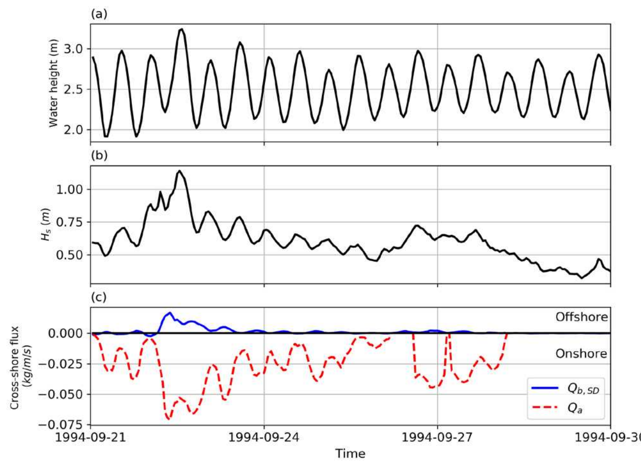

Figure 5. Time series of (a) water height, (b) H_s, and (c) cross-shore bedload flux near of the bar crest at *Sec930* (cross/long-shore positions: 255/930 m). $Q_{b,SD}$ (blue curve on (c)) refers to the bedload flux under combined effects of waves and currents computed according to Soulsby and Damgaard (2005). Q_a (in red on (c)) corresponds to the additional flux linked to the acceleration skewness of waves.

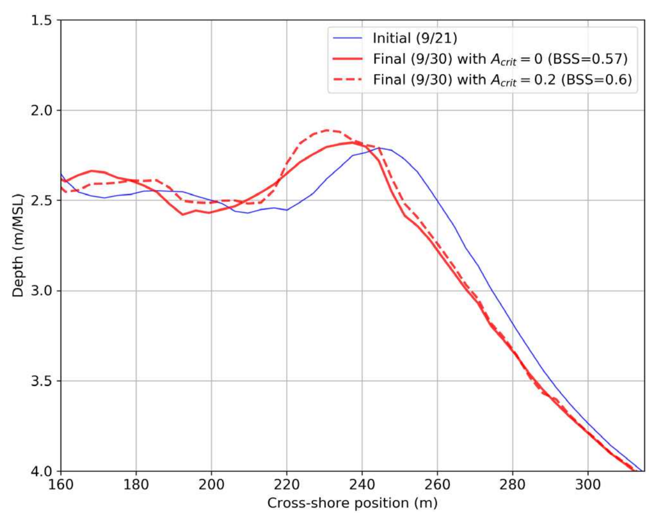

Figure 6. Simulated morphological changes over the 9/21-9/30 period considering different critical acceleration A_{crit} for Q_a estimates (Eq. 1).

CONCLUSIONS

A 3D process-based morphodynamic model coupling sediment transport, currents and waves (vortex force formalism) has been applied to Duck Beach (North Carolina; 1994 experiment) in order to assess its ability to reproduce the cross-shore dynamics of a sandbar. Results underline the necessity of considering an additional sediment flux term associated to acceleration skewness to reproduce the onshore migration of a sandbar during mild wave conditions, although bedload flux estimates already account for wave asymmetry effects (orbital velocity skewness). This motivates further researches based on 3D modelling approach in order to investigate the weight of this additional wave-induced sediment transport on morphological changes occurring in various nearshore environments.

ACKNOWLEDGMENTS

This research was funded by the Fondation de France and Fondation Edouard and Geneviève Buffard. K. Martins greatly acknowledges the financial support from the University of Bordeaux, through an International Postdoctoral Grant (Idex, nb. 1024R-5030).

LITERATURE CITED

Ardhuin, F.; Rascle, N., and Belibassakis, K.A., 2008. Explicit wave-averaged primitive equations using a generalized Lagrangian mean. *Ocean Modelling*, 20(1), 35–60.

Battjes, J.A. and Janssen J.P.F.M., 1978. Energy loss and set-up due to breaking of random waves, *Proc. 16th Int. Conf. Coastal Engineering*, ASCE, pp. 569-587.

Bertin, X.; Fortunato, A.B., and Oliveira, A., 2009. A modeling-based analysis of processes driving wave-dominated inlets. *Continental Shelf Research*, 29(5-6), 819-834.

Dodet, G.; Bertin, X.; Bruneau, N.A.B.; Fortunato, A.B.; Nahon, A., and Roland, A., 2013. Wave-current interactions in a wave-dominated tidal inlet. *Journal of Geophysical Research: Oceans*, 118, 1587-1605.

Dubarbier, B.; Castelle, B.; Marieu, V., and Ruessink, G., 2015. Process-based modeling of cross-shore sandbar behavior. *Coastal Engineering*, 95, 35-50.

Elfrink, B.; Hanes, D.M., and Ruessink, B.G., 2006. Parameterization and simulation of near bed orbital velocities under irregular waves in shallow water. *Coastal Engineering*, 53(11), 915–927.

Elgar, S.; Gallagher, E.L., and Guza, R.T., 2001. Nearshore sandbar migration. *Journal of Geophysical Research: Oceans*, 106(C6), 11623-11627.

Fernández-Mora, A.; Calvete, D.; Falqués, A., and de Swart, H.E., 2015. Onshore sandbar migration in the surf zone: New insights into the wave-induced sediment transport mechanisms. *Geophysical Research Letters*, 42(8), 2869-2877.

Gallagher, E.L.; Elgar, S., and Guza, R.T., 1998. Observations of sand bar evolution on a natural beach. *Journal of Geophysical Research: Oceans*, 103(C2), 3203–3215.

Gallagher, E.; Wadman, H.; McNinch, J.; Reniers, A., and Koktas, M., 2016. A conceptual model for spatial grain size variability on the surface of and within beaches. *Journal of Marine Science and Engineering*, 4(2), 38.

Guérin, T.; Bertin, X.; Coulombier, T., and de Bakker, A., 2018. Impacts of wave-induced circulation in the surf zone on wave setup. *Ocean Modelling*, 123, 86–97.

Guérin, T.; Bertin, X., and Dodet, G., 2016. A numerical scheme for coastal morphodynamic modelling on unstructured grids. *Ocean Modelling*, 104, 45–53.

Hoefel, F. and Elgar, S., 2003. Wave-induced sediment transport and sandbar migration. *Science*, 299(5614), 1885–1887.

Moghimi, S.; Klingbeil, K.; Gräwe, U., and Burchard, H., 2013. A direct comparison of a depth-dependent radiation stress formulation and a vortex force formulation within a three-dimensional coastal ocean model. *Ocean Modelling*, 70, 132–144.

Pinto, L.; Fortunato, A.B.; Zhang, Y.; Oliveira, A., and Sancho, F.E.P., 2012. Development and validation of a three-dimensional morphodynamic modelling system for non-cohesive sediments. *Ocean Modelling*, 57, 1–14.

Ridderinkhof, W.; de Swart, H.E.; van der Vegt, M., and Hoekstra, P., 2016. Modeling the growth and migration of sandy shoals on ebb-tidal deltas. *Journal of Geophysical Research: Earth Surface*, 121(7), 1351-1372.

Roland, A.; Zhang, Y.J.; Wang, H.V.; Meng, Y.; Teng, Y.-C.; Maderich, V.; Brovchenko, I.; Dutour-Sikiric, M., and Zanke, U., 2012. A fully coupled 3D wave-current interaction model on unstructured grids. *Journal of Geophysical Research: Oceans*, 117(C11).

Ruessink, B.G.; Kuriyama, Y.; Reniers, A.; Roelvink, J.A., and Walstra, D.J.R., 2007. Modeling cross-shore sandbar behavior on the timescale of weeks. *Journal of Geophysical Research: Earth Surface*, 112(F3).

Ruessink, B.G.; Ramaekers, G., and Van Rijn, L.C., 2012. On the parameterization of the free-stream non-linear wave orbital motion in nearshore morphodynamic models. *Coastal Engineering*, 65, 56–63.

Sallenger, A.H.; Holman, R.A., and Birkemeier, W.A., 1985. Storm-induced response of a nearshore-bar system. *Marine Geology*, 64(3–4), 237–257.

Short, A.D., 1979. Three dimensional beach-stage model. *The Journal of Geology*, 87(5), 553–571.

Soulsby, R.L., 1997. *Dynamics of Marine Sands: A Manual for Practical Applications*. Thomas Telford, London.

Soulsby, R.L. and Damgaard, J.S., 2005. Bedload sediment transport in coastal waters. *Coastal Engineering*, 52(8), 673–689.

Sutherland, J.; Peet, A.H., and Soulsby, R.L., 2004. Evaluating the performance of morphological models. *Coastal Engineering*, 51, 917–939.

Umlauf, L. and Burchard, H., 2005. Second-order turbulence closure models for geophysical boundary layers. A review of recent work. *Continental Shelf Research*, 25(7–8), 795–827.

Van der Westhuysen, A.J., 2010. Modeling of depth-induced wave breaking under finite depth wave growth conditions. *Journal of Geophysical Research: Oceans*, 115(C1).

Wu, W. and Lin, Q., 2014. Nonuniform sediment transport under non-breaking waves and currents. *Coastal Engineering*, 90, 1–11.

Zhang, Y.J.; Ye, F.; Stanev, E.V., and Grashorn, S., 2016. Seamless cross-scale modeling with SCHISM. *Ocean Modelling*, 102, 64–81.